LWT - Food Science and Technology 153 (2022) 112458

Contents lists available at ScienceDirect

LWT

journal homepage: www.elsevier.com/locate/lwt

Comparative study on the rheological properties of myofibrillar proteins from different kinds of meat

Haifeng Wang [a], Zhi Yang [b,*], Huijuan Yang [c,**], Jing Xue [a], Yunyan Li [a], Shitong Wang [a], Lijun Ge [a], Qing Shen [a,***], Manman Zhang [d,****]

[a] Collaborative Innovation Center of Seafood Deep Processing, Zhejiang Province Joint Key Laboratory of Aquatic Products Processing, Institute of Seafood, Zhejiang Gongshang University, Hangzhou, 310012, China
[b] School of Food and Advanced Technology, Massey University, Auckland, 0632, New Zealand
[c] College of Standardization, China Jiliang University, Hangzhou, 310018, PR China
[d] Department of Neurology, The First Affiliated Hospital of Wenzhou Medical University, Wenzhou, 325000, China

ARTICLE INFO

Keywords:
Myofibrillar protein
Gelation
SDS-PAGE
Viscoelasticity
Microstructure

ABSTRACT

In this study, the gel properties of myofibrillar proteins (MPs) from four meat sources (fish, beef, sheep, and pork) were compared. Oscillatory rheology measurements including temperature sweep, frequency sweep, and strain sweep were conducted to characterise the small and large deformation rheological properties of the MPs. In addition, sodium dodecyl sulfate polyacrylamide gel electrophoresis (SDS-PAGE) and scanning electron microscopy (SEM) were used to evaluate differences in the molecular weight distribution as well as the microstructures in gel among different MPs. Frequency sweep measurements showed that all MP gels were weak gels. MPs extracted from pork exhibited the highest gel strength and most compact gel structure, whereas those from fish exhibited the lowest gel strength and loosest gel structure. In addition, the MP extracted from pork (PSM) had the highest content of myosin heavy chain (MHC) and actin. In conclusion, the MPs extracted from fish source and mammalian sources varied significantly in terms of rheological properties and microstructural characteristics. These results provided useful information for developing mixed gel products with different gel strengths.

1. Introduction

Meat is a vital component of a balanced diet, and it is the main source of essential proteins, fats, iron, vitamin B_2, and other nutrients for humans (Li et al., 2020a). In China, the proportion of people consuming meat products, particularly pork, is high, accounting for 55%–65%, and meat consumption is increasing annually (Grunert, 2006). With economic development, the development of new meat products has become a research hotspot (Gabdukaeva, Gumerov, Nurgalieva, & Abdullina, 2021).

Protein is one of the most important constituents of meat products (Mahmudul et al., 2021). According to the solubility of proteins in different solutions, they can be divided into three categories: salt-soluble proteins [myofibrillar protein (MP)], water-soluble proteins (sarcoplasmic protein), and insoluble proteins (muscle stromal protein) (Ahhmed, Kuroda, Kawaharas, & et, 2009). MP is a mixed protein system consisting of myosin, actin, actomyosin, and two or three regulatory structural proteins (Sano, Noguchi, & Tauchiya, 1988). It is the main muscle protein group (50%–55%), which imparts the functional characteristics to meat products (Yang, Zhong, & Sun, 2021). In meat processing, MP determines the formation of a three-dimensional gel network during the heating treatment (Li, Fu, Zhao, et al, 2020). Heat-induced gelation of MP is a complex thermodynamic process. First, the globular head of myosin starts coagulating at a low temperature (30 °C–45 °C). Thereafter, the tail of the spiral rod begins to expand and aggregate when the temperature is further increased from 55 °C to 85 °C. Finally, if the concentration of MP exceeds the critical protein concentration for gelation, the aggregates are cross-linked to form a

* Corresponding author.,
** Corresponding author.
*** Corresponding author.
**** Corresponding author.
E-mail addresses: z.yang2@massey.ac.nz (Z. Yang), huijuanyang2012@gmail.com (H. Yang), leonqshen@163.com, sq@zjgsu.edu.cn (Q. Shen), zhangmanman@wmu.edu.cn (M. Zhang).

https://doi.org/10.1016/j.lwt.2021.112458
Received 2 May 2021; Received in revised form 4 September 2021; Accepted 11 September 2021
Available online 12 September 2021

well-spanned gel network (Wang et al., 2014). The gelation process can be monitored using oscillatory rheology, which applies a small deformation to avoid disruptions of the gel network (Antonov & Zhuravleva, 2019). To date, the structure and gelation mechanism of MP from pork have been widely studied. Various physical modification strategies such as ultrasound treatment (Li, Li, Kang, et al, 2020), microwave heating (Wei et al., 2020), pre-treating by high pressure (Fidalgo, Saraiva, Aubourg, & Vázquez, 2020), as well as chemical modification methods, such as transglutaminase cross-linking, have been used to enhance gel strength (Yang & Zhang, 2019; Cao et al., 2019). Moreover, multiple modification methods including addition of sodium pyrophosphate coupled with catechin (Cao, Ma, Huang, & Xiong, 2020) or NaCl with chloride salt mixtures (Dai et al., 2021) have been employed to improve the gel strength of pork. However, most of these studies have focused on the MP extracted from pork (Lee & Chin, 2019; Jiang & Wu, 2018) and chicken (Chen, Qiu, Chen, Li, & Liang, 2020; Xu, Zhao, Wei, et al, 2020), and only a few studies performed comparisons of MPs from different meat sources, especially fish and mammals (Malva et al., 2018). In this study, we systematically studied the differences in rheological properties between fish source MP – FSM and mammalian sources MP (beef source MP - BSM, sheep source MP – SSM, and pork source MP – PSM) at the concentrations of 10, 20, and 30 mg/mL, to provide a reference for the modification of FSM in the future research. Small and large deformation rheological properties of different MP gels that were induced from thermal treatment were characterised. The protein compositions and microstructures of the MP gels were characterised by sodium dodecyl sulfate polyacrylamide gel electrophoresis (SDS-PAGE) and scanning electron microscopy (SEM), respectively. The detailed physicochemical characterisation of MPs from different animal species was performed to elucidate the gelation mechanism of MPs and provide insights into the development of novel MP ingredients or meat products.

2. Materials and methods

2.1. Materials

Back meat of white croaker frozen surimi was purchased from Zhejiang Yufu Food Co. Ltd. (Hangzhou, China), the longissimus dorsi muscles of cow (cattle breeding with Australian Valley in Australia), sheep (Tan sheep in Yanchi County of Ningxia, Ningxia China), and pork (black pig in Taihu, Jiangsu, China) were purchased from a local market (Xinxiang Gaojin Food co. LTD, Zhejiang, China). The fish and animals were aged 180 ± 3 days, and they were frozen after slaughtering for 24–48 h.

Bradford protein kit and SDS were purchased from Shenggong Bioengineering Co. Ltd (Shanghai, China). Pre-stained protein marker was purchased from Solar-bio company (Beijing, China). The Coomassie brilliant blue R250 (electrophoretic grade) was purchased from Ruji Biotechnology Co. Ltd (Shanghai, China). All chemicals and reagents including potassium chloride, tris (hydroxymethyl) methyl aminomethane, maleic acid, and Biuret A and B were of analytical grade and purchased from Aladdin Co. Ltd (Shanghai, China). These chemicals and reagents were used without any further purification.

2.2. Preparation of meat pieces

The four types of raw meat were minced using a meat grinder (HCP-A6 Grinder, Hattiecs, China) to form 3 mm pieces, and then washed with deionised water under stirring at 6000 rpm for 5 min. After that, those meat pieces were further rinsed with 0.15% NaCl solution to remove most of the fat and some of the water-soluble proteins. Temperature was maintained below 10 °C during the entire process.

2.3. Preparation of MPs

The samples were prepared according to the method of Wang et al. (2020), with minor modifications, as shown in Fig. 1. Briefly, 40 g minced meat was weighed, and 10 times volume of buffer A (50 mM KCl–20 mM tris maleate, pH 7.0) was added. The suspension was mixed and homogenised (90,000 rpm) at 4 °C using an Ultra-Turrax homogeniser (T-18, IKA, Germany). The samples were allowed to stand for 15 min before centrifugation at 8000×*g*, 4 °C for 5 min (Hettich Rotina 420R, Hettich, Germany) to obtain the precipitate. The aforementioned procedures were repeated twice to obtain the protein mixture. Further, 10 times volume of buffer B (0.6 M KCl-20 mM Tris maleate, pH 7.0) was added to the samples and the suspension was mixed and homogenised. Further, the extraction was performed for 1 h before centrifugation (8000×*g*, 4 °C, 10 min) to obtain the supernatant containing MPs. Finally, the supernatant was washed with four times volume of pre-cooled (4 °C) deionised water, and the MPs were obtained through centrifugation (6000×*g*, 10 min). The obtained MPs were dissolved in 0.6 M KCl solution, and their concentrations were determined using the Biuret method (Wang et al., 2020). Based on the protein determination results, solutions with protein concentrations of 10, 20 and 30 mg/mL were prepared (Gornall, Bardawill, & David, 1949).

2.4. Determination chemical compositions of meat pieces

Chemical compositions of meat pieces from the four different sources were determined using the method of Zhou, Liu and Zhu (2020). The moisture content was determined by drying at 105 °C until reaching constant weight; ash content was determined using the muffle furnace volatilisation method; and total fat and total protein contents were determined using Soxhlet extraction and Kjeldahl methods, respectively (Zhou et al., 2020). The MP content refers to the ratio of MP extracted from 40 g minced meat using the method in Section 2.3 to the total protein content in the minced meat.

2.5. Electrophoretic analysis

SDS-PAGE was performed according to the method of Laemmli (1970) by using 10% separation gel and 4% concentrating gel with a discontinuous buffer system under reducing conditions. The myofibrillar fractions were diluted in SDS sample buffer (8 M Urea, 20 mM Tris, 2% SDS, 2% β-mercaptoethanol, pH 8) to obtain the protein concentration of 1 mg/mL in a test tube. The mixtures were incubated for 6 h at 4 °C to allow protein dissociation and centrifuged at 5000 rpm for 3 min to remove insoluble particles. Following this, the mixture was boiled for 5 min and centrifuged again at 5000 rpm for 3 min to remove insoluble particles. Pre-stained Protein Marker (20–220 kDa) was used as the protein standard for the estimation of molecular weight of the samples. Aliquots of the sample (15 μL) were loaded onto each lane. The electrophoresis was performed at a constant voltage of 70 V until the protein molecular weight ran out of the concentrated gel, and further, a constant voltage of 110 V was applied until the electrophoresis was completed. After separation, the gels were stained using 0.4% Coomassie brilliant blue R-250 for 45 min and decolorised in deionised water including 7.5% acetic acid and 5% methanol until the protein bands appeared clearly. The electrophoresis pattern was analysed using the Gel-Pro Analyzer (Bio-Rad, USA).

2.6. Rheological characterisations

All rheological measurements were conducted using a stress-controlled rheometer (MCR 302, Anton Paar, Graz, Austria) equipped with a parallel plate geometry (50 mm diameter, angle 0°, gap 0.5 mm) according to the method of Liu, Liu, and Luo (2015). The samples were transferred onto the bottom plate of the rheometer, and the edge of the samples was covered with liquid paraffin to prevent dehydration during measurements. Before measurements, the samples were stabilised at 10 °C for 3 min, and subsequently, they were subjected to the temperature sweep, frequency sweep, and strain sweep tests. These

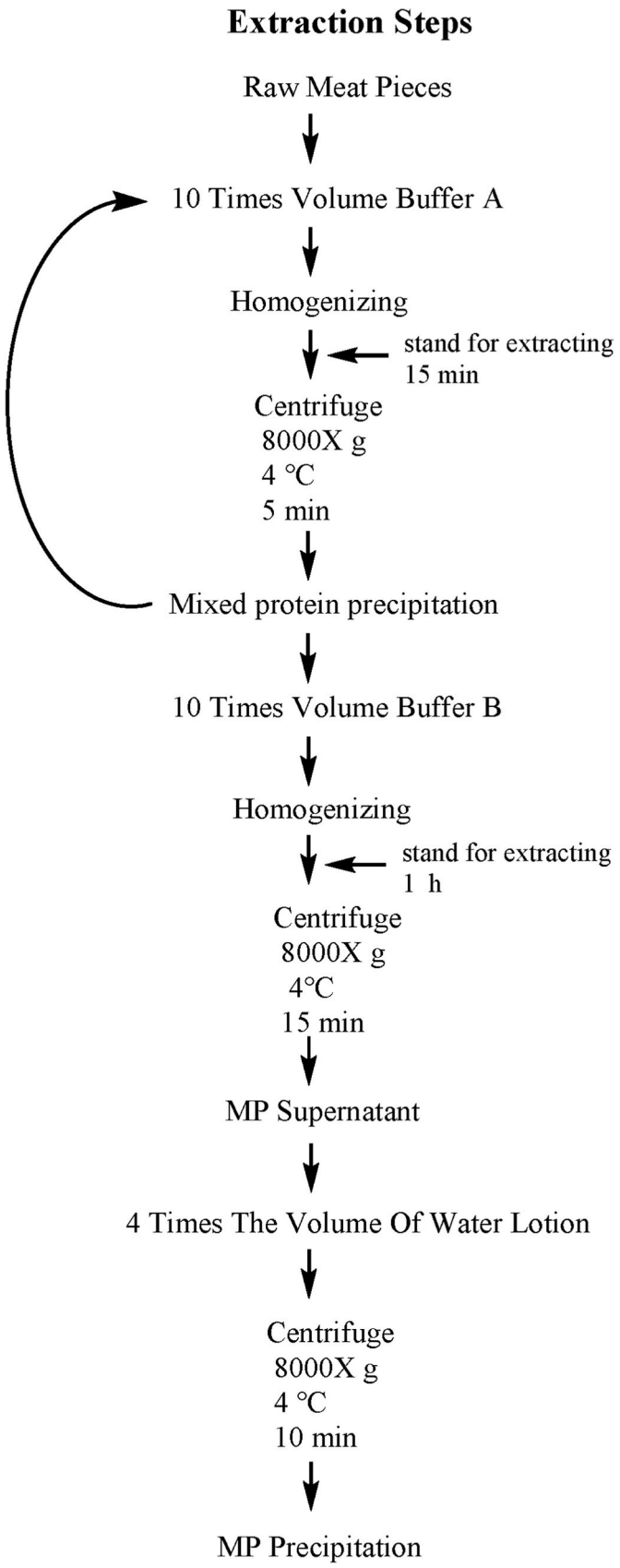

Fig. 1. Detailed experimental extraction procedures for extraction of MPs from different meat sources.

measurements were performed on the same sample. All the rheological tests were performed in triplicates on the three samples.

The sol–gel transitions of the four MPs at three concentrations were investigated using temperature sweep tests, where G' and G'' were monitored at a frequency of 1 Hz and strain amplitude of 1%, with temperature increasing from 10 to 85 °C at a heating rate of 1 °C/min. After temperature sweep, the samples were maintained at 85 °C for 10 min, followed by a frequency sweep measurement conducted in a frequency range of 0.1–100 Hz and at 1% strain to probe the viscoelastic behaviour of samples. The frequency sweep measurements were conducted at an amplitude strain of 1% within the linear viscoelastic region (LVR). Finally, the strain sweep tests were performed at a strain amplitude (0.01%–10000%) and a frequency of 1 Hz to study the large deformation rheological characteristics of the MP gels.

2.7. Scanning electron microscopy (SEM)

MP gel samples at 30 mg/mL were prepared according to the procedure described in Section 2.4. The MP samples were heated in an electric-heated water bath (DK-S12, Experiment Instrument Co. Ltd., Shanghai) at 85 °C for 45 min. After gelation, the samples were immediately immersed in an ice-water bath for 5 min. Thereafter, the gels were frozen at −80 °C for 4 h before lyophilisation using a freeze dryer (Songyuan Huaxing LGJ-10, Beijing). The dried samples were slowly frozen in liquid nitrogen and were sliced (thickness, 2–3 mm) using a razor blade. The samples were subsequently sprayed with gold by using a sputter coater for 40 s (Q150T, Quorum, England). Finally, the microstructure of various meat gels was examined using a field emission scanning electron microscope (Regulus 8100, Hitachi, Japan).

2.8. Statistical analysis

All experiments were performed in triplicates. The representative rheological results were selected to present. The data of other tests were represented as the mean ± SD, and SPSS 21.0 software (IBM Corporation, NY, USA) was conducted to analyse the results with a one-way ANOVA ($p < 0.05$). The difference between least-square means was performed using Duncan's multiple range test.

3. Results and discussion

3.1. Chemical composition of the four types of meat

Proximate analysis was conducted to gain in-depth understanding of the nutritional value of meat products and provide effective dietary basis to consumers. The nutritional compositions of meat vary with animal species, age, location, and degree of fat and lean (Wood et al., 2008).

The chemical compositions were found to differ significantly among

Table 1
Chemical compositions of four types of meat pieces (fish, beef, sheep, pork).

Index	Fish	Beef	Sheep	Pork
Water content (g/100g)	76.20 ± 0.21^{c**}	78.59 ± 0.07^{b**}	78.35 ± 0.66^{b**}	79.73 ± 0.31^{a**}
Ash content(g/100g)	0.60 ± 0.10^{a*}	0.53 ± 0.35^{b**}	0.55 ± 0.01^{b**}	0.41 ± 0.15^{c**}
Total fat(g/100g)	1.73 ± 0.04^{c**}	2.14 ± 0.17^{b**}	2.94 ± 0.08^{a**}	2.82 ± 0.23^{a**}
Total protein(g/100g)	17.13 ± 0.13^{b*}	15.94 ± 0.20^{c**}	14.01 ± 0.50^{d**}	18.92 ± 0.39^{a**}
MP content(g/100g)	13.45 ± 0.50^{b*}	11.04 ± 0.50^{c**}	10.56 ± 0.50^{c*}	15.16 ± 0.39^{a*}

Note: Data are given as mean values ± standard deviation ($n = 4$). Different letters within the same row indicate significant differences ($p < 0.05$) between mean values. "**"indicates that there is a significant correlation at the $p = 0.01$ level.

different meat sources ($p < 0.05$; Table 1). Moisture, ash, and total fat contents in all the MP samples were in the range of 76–80, 0.4–0.6, and 1–3 g·100 g^{-1}, respectively. In terms of the total protein content and MP content, the order was: pork source pieces (PSP) > fish source pieces (FSP) > sheep source pieces (SSP) ≈ beef source pieces (BSP).

The difference in the chemical composition among the MPs was related to the chemical composition of the original sample. The results showed that the moisture and ash contents in BSP and SSP samples were similar, whereas the fat content in SSP was higher than that in BSP, and this result was consistent with previous studies conducted by Hess, Moss and Rule (2008). Among the four samples, the total protein and MP contents were the highest in PSP, and the result is in agreement with a previous study performed by Komprda, Zelenka, Fajmonova, Bakaj, and Pechova (2003). Results showed that the chemical composition varies, particularly in term of protein content, in different meat sources.

3.2. SDS-PAGE analysis

The processing of meat products is closely related to the protein composition (Cai, Wan, Li, & Li, 2020). To understand the components of different meat proteins, SDS-PAGE was used to analyse the protein patterns (Jia et al., 2019). Under reducing conditions, proteins were disrupted, unfolded, and stretched, and intramolecular disulphide bonds were destroyed. The separation of different proteins was performed in exclusion gels with limited diffusion, and high-resolution narrow protein bands were obtained.

As shown in Fig. 2A, the main MP bands in the four types of MPs were: myosin heavy chain (MHC; 220 kDa), paramyosin (100 kDa), actin (43 kDa), tropomyosin (37 kDa), and three myosin light chains (MLC; 15, 17, 24 kDa). The results were consistent with those reported by Lametsch (2004) and Cort (2008). According to the molecular weight distribution of proteins, in FSM, the 33.0 kDa content was the highest (11.55% higher than that in BSM) but the paramyosin content was only 1.3% and tropomyosin was almost 0%. In BSM, the MLC content was high (13.71%), and the paramyosin content was low (4.78%). In SSM, the MLC content was the highest (25.86%), but the tropomyosin content was the lowest (10.75%). In PSM, the MHC content was the highest (51.11%), and it had a unique band of 57 kDa molecular weight. In all the groups, except for FSM, the most intense band was MHC, followed by actin. In FSM, the most intensive band was tropomyosin, followed by actin. These results were consistent with a previous study (Bhat, Morton, Mason, & Bekhit, 2019).

In terms of protein bands, FSM exhibited only a few protein bands, and this result deviated from the previous results on the MP contents. In terms of protein band width, the band of PSM was the widest and that of BSM was the narrowest, indicating the least molecular weight distribution; this result was in a good agreement with a previous study conducted by Zilhadia (2013).

3.3. Small and large deformation rheological properties of MP gels

The rheological properties of MPs gels from four different meat sources were investigated. Results obtained from rheological measurements can be used to understand protein interactions and aggregations during the heating (Romani, Machado, Olsen, & Martins, 2018).

3.3.1. Thermally induced gelation

One of the most important properties of MPs is their gelling property, which is critical in many food applications (Zhou, Yang, Wang, Wei, & Li, 2018). The changes in the dynamic viscoelastic properties of the four types of MPs at three concentrations during the heating were determined by monitoring storage modulus (G') and loss modulus (G''), which were found to be temperature dependent, as shown in Fig. 3. The change of the G' and G'' in MPs during the heating process implied the opening, unfolding, of the protein structure and indirectly reflected the process of protein denaturation, aggregation, and spatial network formation (Miller, Acevedo, Lonergan, Sebranek, & Tarté, 2019).

The changes of G' as function of temperature for all MP samples showed three stages, as shown in Fig. 3 (Xu, Zhao, et al., 2020): 1) the initial increase in G' (gel setting) corresponding to cross-linking of the myosin molecules through head–head interactions (Miller et al., 2019); 2) the decrease in G' due to denaturation and dissociation of MLC (gel weakening) and an increase in the fluidity of the filaments; and 3) a second increase, resulting from the cross-linking of myosin through tail-to-tail interactions (gel strengthening). However, the three stages of G' for MPs from different sources were different, especially for FSM, which displayed a slightly downward trend from 10 to 30 °C. This phenomenon was also observed by Westphalen, Briggs, and Lonergan (2006), who reported that when the temperature was below 30 °C, the hydrogen bond was the main force in maintaining the integrity of MPs (Westphalen et al., 2006). With an increase in temperature, the hydrogen bonds were weakened, leading to a decreased G' (Baune, Schroeder, Witte, Heinz, & Terjung, 2021). This behaviour was also reported by Lin, Zhang, Li et al. (2019) who studied the effect of nano fish bone on myosin gel properties of silver carp. At 30–38 °C, G' increased because of a certain degree of cross-linking between the internal protein molecules were formed. This led to the formation of three-dimensional network structures, implying the transition from sol

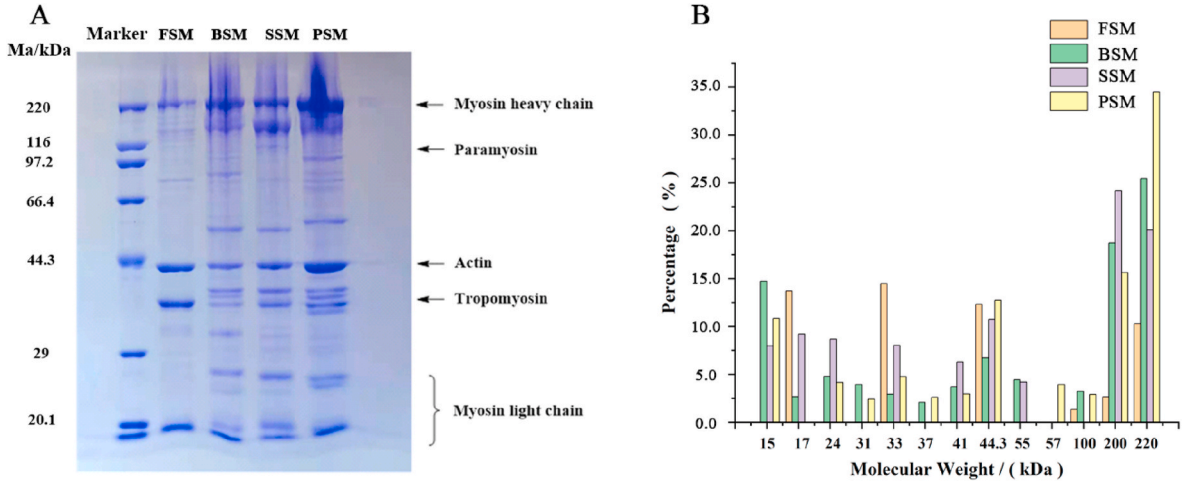

Fig. 2. (A) SDS-PAGE patterns of different MPs extracted from four types of meat sources (fish, beef, sheep, pork) and (B) percentages of each band in SDS-PAGE patterns obtained from the densitometry analysis of the gel pattern.

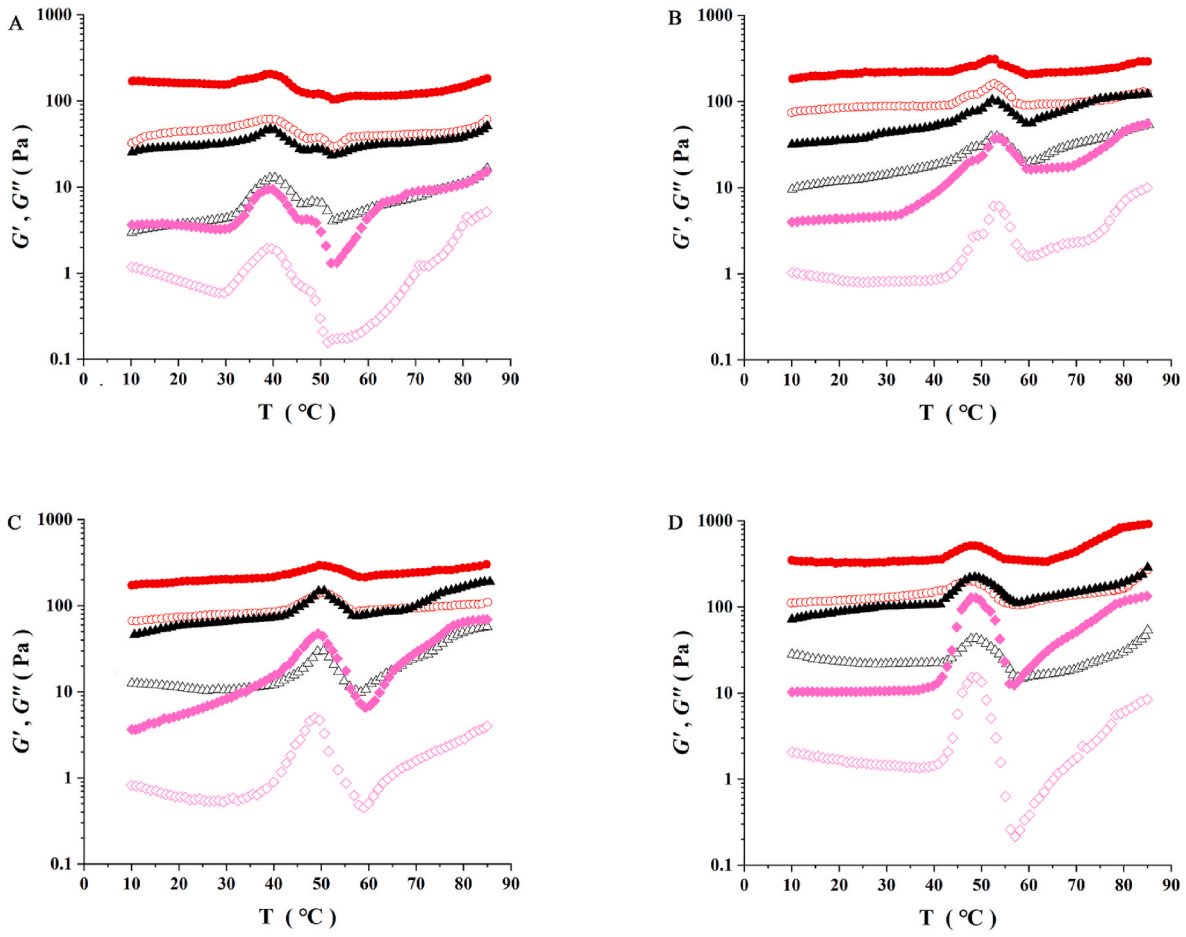

Fig. 3. Storage modulus (G', solid symbols) and loss modulus (G'', empty symbols) as a function of temperature during a rheological temperature sweep from 10 to 85 °C for MPs extracted from four types of meat sources (fish, beef, sheep, pork) at three concentrations. A. Fish MP gel; B. Beef MP gel; C. Sheep MP gel; D. Pork MP gel. Spheres: 30 mg/mL, triangles: 20 mg/mL, diamonds: 10 mg/mL.

to gel. Afterwards, the G' decreased sharply around 38–51 °C, indicating that the rod-shaped part of the myosin tail was broken and was in a relaxed state, which impaired the integrity of protein network structures (Sano et al., 1988). Finally, the G' increased until the end, which indicated that a stable gel structure was gradually generated (Zhou et al., 2020).

The G' versus temperature curves of MP samples from the other three meat sources were similar; the G' increased from 10 °C to the first peak and downwards until the gelling point and then were again upwards. The increase in G' was correlated to the protein interaction; with increasing temperature, protein molecules unfolded slightly, and the weaker interaction led to a small increase between 10 °C and 33 °C. In contrast, when the temperature was between 33 °C and 43 °C, the curves rose sharply. This trend was explained by the uncovering of the α-helix structure of myosin and the exposure of sufficient active groups, such as hydrophobic region and active sulfhydryl group (Romani et al., 2018). Subsequently, with further increase in temperature, the gel networks weakened. In this process, the values of G' declined significantly. This could be attributed to MLC, the main part of MP, which began to denature, and the tail of myosin in the MP, which began to untwist, destroying the integrity of protein network structure and leading to the enhancement of fluidity and partially damage the network structure of the entire protein (Zhou et al., 2015; Westphalen et al., 2006; Sano et al., 1988). In addition, some studies have showed that the decrease in G' might be attributed to the intramolecular damage of protein. When the protein helix was changed into a conical shape, the mobility of the gel network increased markedly, thus destroying the protein network structure (Chen et al., 2016). However, the G' of BSM only decreased slightly, indicating the slight stretches of the protein chain. This finding indicated that the flexibility of BSM was not significantly affected by temperature (Fu, Liu, Wang, Hua, & Song, 2019). When the temperature was further increased, the molecules were unfolded, the active group was exposed, and the protein began to aggregate, precipitate, and crosslink. Finally, the structure of the protein network was rebuilt (Shan et al., 2020). The rigidity of the gel network structure was also increased, which can be mainly attributed to the disulfide bonds, hydrophobic interactions, and the irreversible cross-linking of myosin (Zhang, Li, Shi, Zhu, & Luo, 2017). Similar rheological behaviours have been reported in previous studies (Baune et al., 2021; Chen et al., 2016; Fu et al., 2019).

With an increase in temperature, the G' values of all the samples increased, with the peak values appearing at the temperature of 35–55 °C, indicating the formation of a highly elastic gel network. This result was consistent with that reported by Wang (2014). Notably, the G' curves of SSM and PSM had only one peak, whereas G' curves of FSM and BSM showed two peaks. The peaks of FSM were more prominent than those of BSM. Zheng, Han, Ge, Zhao, and Sun (2019) suggested that the gelation might be due to the denaturation and aggregation of myosin heads. We speculated that in this temperature range (35–55 °C), when the MP molecules were deformed and aggregated, the heads of myosin (the main functional group of MP) were denatured and combined with the tail of untwisted myosin. Due to the difference between the head and tail of myosin in terms of thermal stability, the temperatures required for generating the network structure were different, which led to differences in the number of peaks in G' curves. Similar results were observed in the study conducted by Consoli et al. (2018). The authors reported that the

samples showing only one peak in the temperature sweep curve have a more stable and compact gel structure than the samples showing multiple peaks. Additionally, the peaks of BSM and PSM samples appeared at higher temperatures (45–55 °C), implying the unfolding and association of myosin globular heads. The peak G' values of SSM and FSM were obtained at a relatively lower temperature (35–45 °C), indicating that their MPs denatured at an earlier stage and showed poor thermostability (Hrynets, Ndagijimana, & Betti, 2014).

The G' value curves of the four types of MP samples at three concentrations were ordered from higher to lower concentrations, suggesting that a high concentration could promote the thermal aggregation of MPs during heating. With increasing in the protein concentration, the maximum gelation temperatures also increased to higher values. This phenomenon indicated that the greater packing density of protein molecules could enhance proteins interaction, resulting in a greater steric hindrance. Therefore, the protein was unfolded at a high temperature. This finding agreed well with a previous study (Eyjurskarð, Haug, Elharfaoui, Djabourov, & Draget, 2009).

3.3.2. *Small deformation rheological properties*

Frequency sweep provides knowledge of the network structure. The G' and G'' as a function of frequency for each sample is shown in Fig. 4. All the samples displayed an interconnected gel-like network structural characteristics in which G' and G'' only slightly increased with an increase in frequency, demonstrating a weak dependence on frequency. Furthermore, the value of G' was higher than that of G'' over the whole frequency range, indicating an elastic-dominant behaviour (Wang et al., 2019; Yang et al., 2016).

In general, the dispersion systems can be divided into four categories: a dilute solution, an entangled network (or concentrated solution), a weak gel, and a strong gel (Xu, Xu, Zhang, & Zhang, 2008). Based on the frequency sweep results, all the samples could be classified as weak gels, indicating that their abilities to form weak associations and gel networks. In addition, the frequency dependence indicated that the gel-like network may consists of non-covalent physical crosslinks, which was also reported by Tang and Liu (2013).

It can be seen from Fig. 4 that differences between values of G' and G'' significantly increased with an increasing in protein concentrations, indicating a gradual increase in the gel strength at high concentrations. In terms of the MP sources, the order was: FSM < SSM ≈ BSM < PSM. The value of G' at 1 Hz for all the samples are plotted in Fig. 5 A to allow easy companions. For the MP from all meat sources, G' increased with the protein concentrations. Furthermore, at all protein concentrations, G' was the highest in PSM while the lowest in FSM. As shown in SDS-PAGE, BSM, SSM, and PSM had a greater amount of MHC (220 kDa), which had a highly ordered macromolecule structure and could promote the entanglement of the MP chains. Therefore, the rigidity of BSM, SSM, and PSM, particularly of PSM was higher than that of FSM. This might indicate that the protein network structures of BSM, SSM, and PSM were denser than that of FSM after gelation (Elif, Ebru, Hichem, Senol, & Figen, 2020). These results might be related to strong protein–protein interactions leading to a more entangled network (Huang et al., 2019). Shi, Zhou and Wang (2021) validated that the self-aggregation of myosin could predominantly contribute to the gel network.

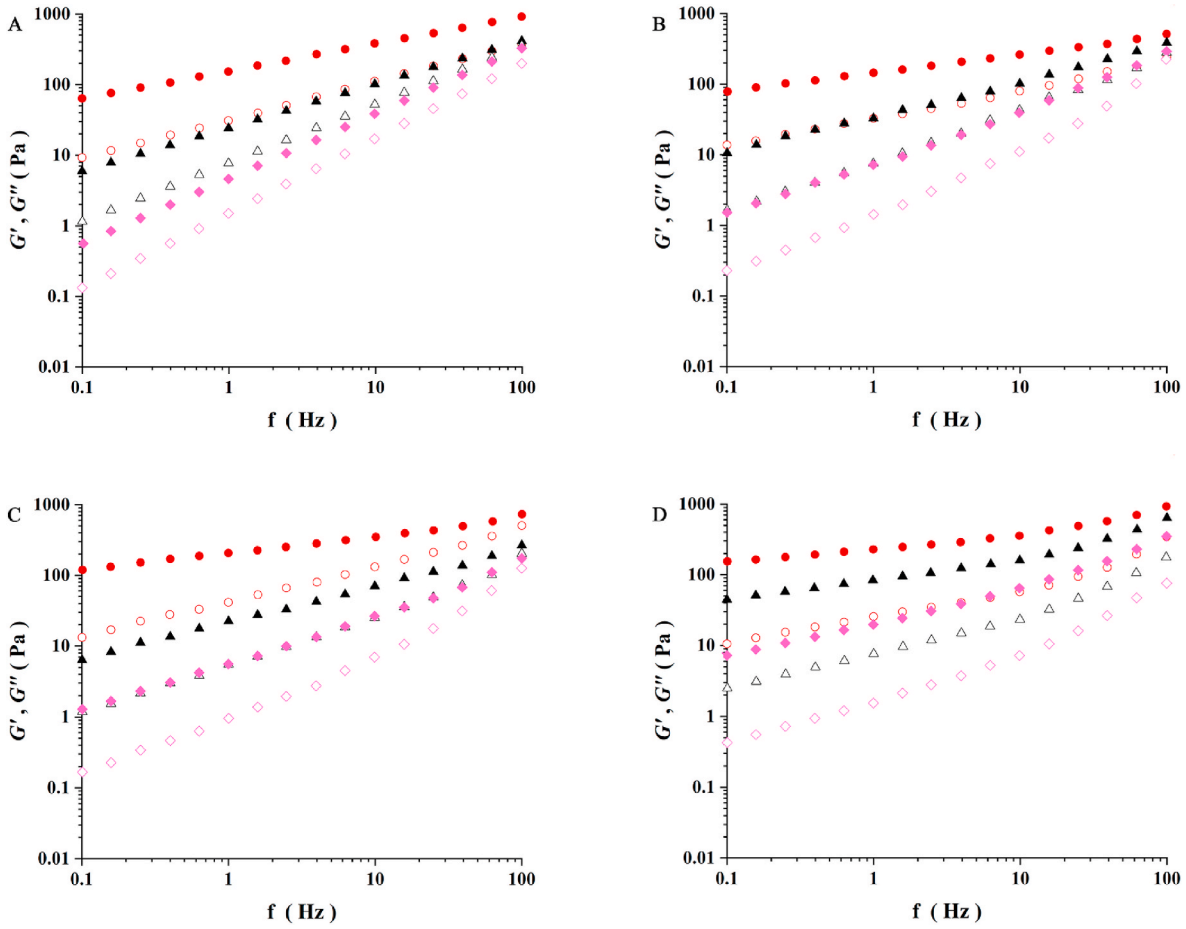

Fig. 4. Dependence of Storage modulus (G', solid symbols) and loss modulus (G'', empty symbols) as a function of frequency for different MPs extracted from four types of meat sources (fish, beef, sheep, pork) at three concentrations. A. Fish MP gel; B. Beef MP gel; C. Sheep MP gel; D. Pork MP gel. Spheres: 30 mg/mL, triangles: 20 mg/mL, diamonds: 10 mg/mL.

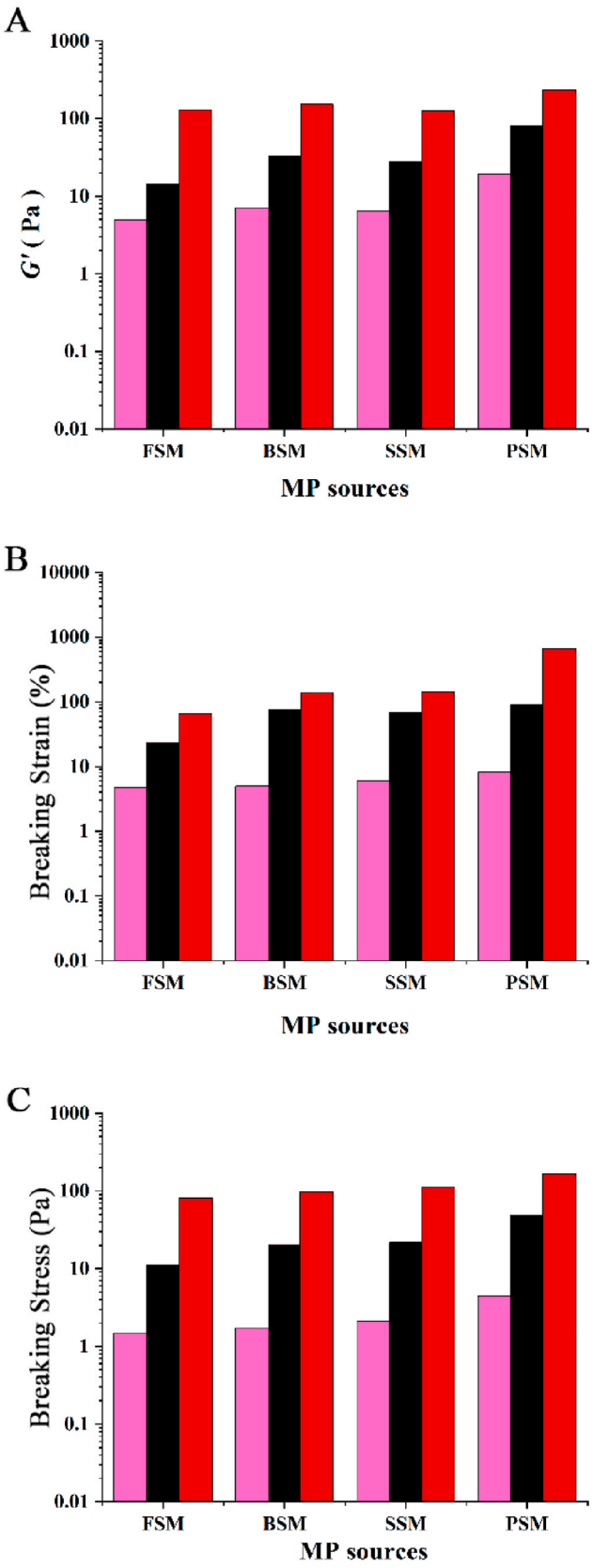

Fig. 5. The storage modulus G' at 1 Hz from the linear viscoelastic regions (A), breaking strain values (B), and breaking stress values (C) for MPs extracted from four types of meat sources (fish, beef, sheep, pork) at various protein concentrations. Red columns: 30 mg/mL, black columns: 20 mg/mL, magenta columns: 10 mg/mL.

3.3.3. *Large deformation rheological properties*

The dynamic strain sweep measurement was used to determine structural changes in MP gels under large deformations. Dynamic strain sweep curves of the four types of MPs at three concentrations are shown in Fig. 6. For all the MP samples, the G' dominated over the G'' in the Linear Viscoelastic Region (LVR) until the critical strain, indicating a solid-like response of the gel (Raei, Rafe, & Shahidi, 2018). The limit of LVR was different depending on protein sources and concentrations; the PSM had the longest LVR, and the higher concentration of samples led to higher modulus values. This because the aggregation suspensions at high concentrations contained more solutes and exhibited a highly stable structure and great elasticity (Zhu, Li, & Wang, 2018). With a further increase in the strain amplitude beyond the critical strain value, G' of all the samples decreased rapidly, indicating a breakdown of bonds in the gel network. In addition, Siong, Rodney, Christopher, Samson, and Li (2014) reported that high critical strain values indicated a strong tolerance to deformation and a stable intermolecular structure in protein samples. Higher critical strain values were identified for all the samples at greater protein concentrations, and the values of critical strain were in the order: PSM > BSM ≈ SSM > FSM. Therefore, PSM was the best gelling sample in terms of the gel strength compared with other samples (Siong et al., 2014). This finding might be explained by the greater degree of connectivity between molecules and close interactions in the PSM, which resulted in the formation of highly structured and stable systems (Anvari & Joyner, 2017).

With further increase in the strain amplitude, the values of G' and G'' cross-overed. The corresponding crossover strain and stress points are shown in Fig. 5 B and C, which indicated that the viscoelastic solid transited to the viscoelastic fluid. At this strain, the value of G'' reached its maximum, which implied that a sufficient number of physical bonds was destroyed, and maximum energy was dissipated (viscous response). The moduli of intersections had the same order as the values of critical strains, which further illustrated that PSM had the strongest structural rigidity. Finally, when the strain amplitude exceeded the G' and G'' crossover point; G'' started to dominate G'. This indicated that the gel was destroyed, and the mobility was enhanced. (Day, Xu, Oiseth, Lundin, & Hemar, 2010; Wang et al., 2019). Generally, the variation of breaking strain and breaking stress with types of MPs followed a similar trend as G' (1 Hz) (Fig. 5), implying the large deformation rheological properties agreed well with the small deformation viscoelastic characteristics.

3.4. *Microstructures revealed by SEM*

Microstructures of MP gels from various meat sources were characterised by SEM and micrographs were shown in Fig. 7. There were a few number of pores within the gel network and fine filamentous fibres could be observed. The morphology of filaments may be affected by the size and shape of the proteins (Li, Wang, Liu, et al, 2019). The surface of pork MP gel was smoother than that of the other three gels and showed the most compact protein structures. Meanwhile, compared to the other three MP gels, a large porosity can be observed in the micrographs of fish MP gels, which had rough surface with loose protein network structures. This result agreed well with the rheological findings, and the weakest gel strength of FMP gel could be explained by its highly rough and more open protein networks with large voids. Furthermore, the gel structure of BSM was found to be similar to that of SSM. The sheep MP gel exhibited fewer and smaller pores than the beef MP gel, which validated the results described in Section 3.3. However, the filamentous fibre network of beef MP gel was more complex than the sheep MP gel. Lin, Li and Zhou (2021) reported that both weak hydrophobic interactions and inferior protein oxidation could lead to disordered aggregation of the protein, resulting in the formation of a loose and irregular gel network. Shi, Zhang, Zhang, et al (2021) reported the effect of ultrasound pre-treatment on the nutritional and structural properties of MPs extracted from chicken breast and also indicated that strong

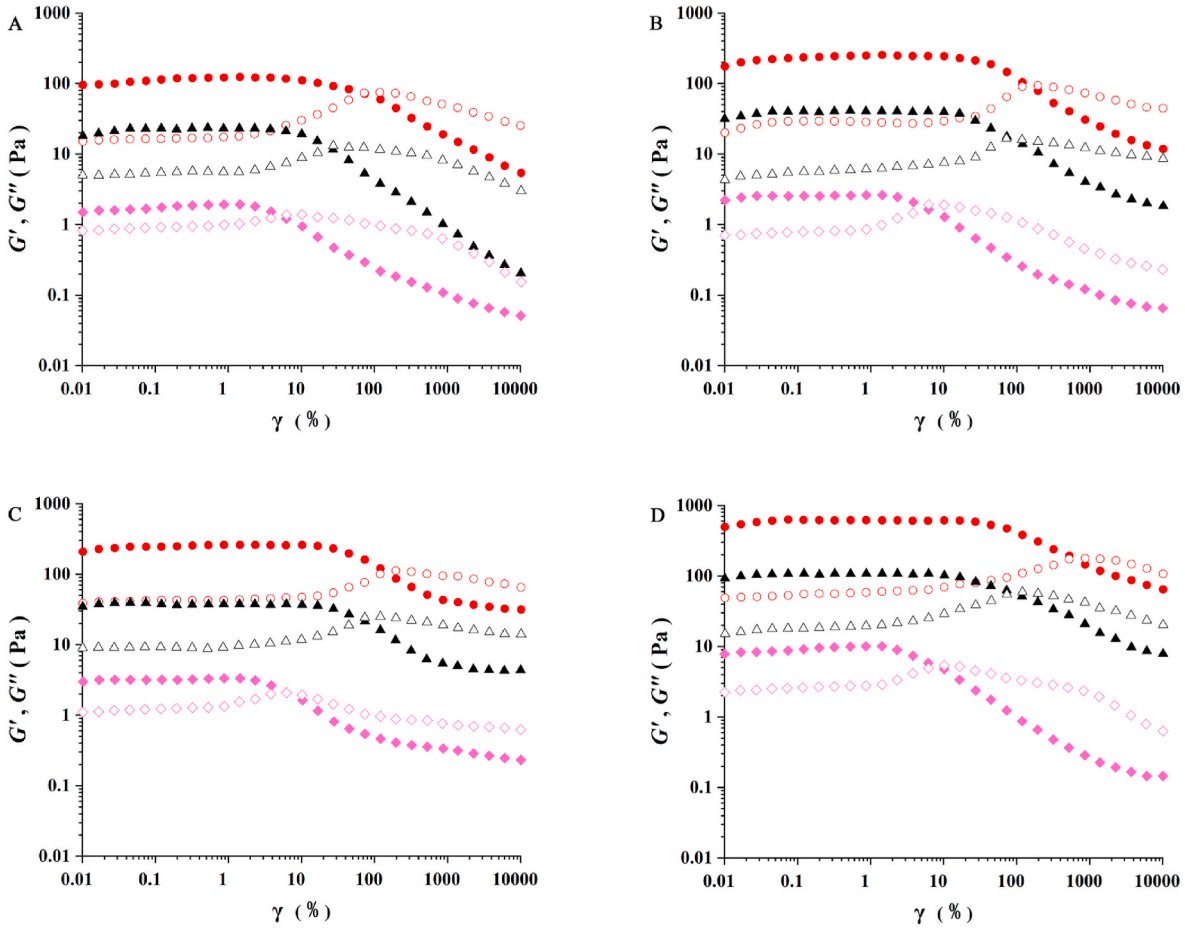

Fig. 6. The dependence of strain amplitude on storage modulus (G', solid symbols) and loss modulus (G'', empty symbols) for different MPs extracted from four types of meat sources (fish, beef, sheep, pork) at three concentrations. A. Fish MP gel; B. Beef MP gel; C. Sheep MP gel; D. Pork MP gel. Spheres: 30 mg/mL, triangles: 20 mg/mL, diamonds: 10 mg/mL.

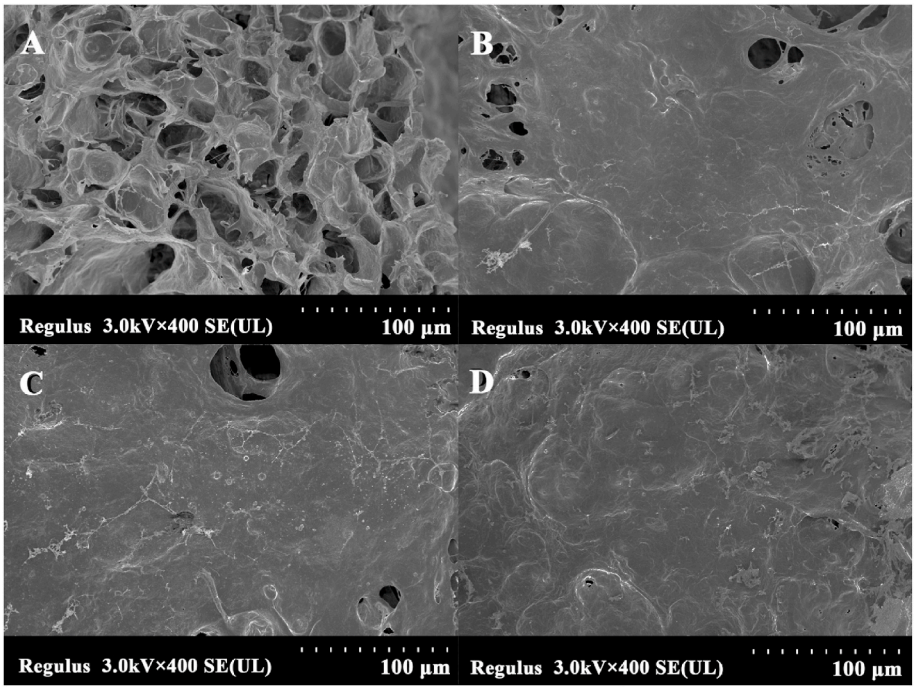

Fig. 7. Scanning electron microscopy (SEM) images of MP gels from four kinds of meat sources (fish, beef, sheep, pork) at 30 mg/mL. A. Fish MP gel; B. Beef MP gel; C. Sheep MP gel; D. Pork MP gel.

hydrophobic interactions between protein molecules could yield a strong and highly compact gel structure. In summary, the microstructure of the MP gels from different meat sources correlated well with their rheological properties. The gels demonstrating compact and dense packing networks with small number of voids resulted in the stronger gel strength (PSM), while the inferior mechanical properties were due to the thinner protein filaments or strands and more loose protein networks with large porosity (FSM).

4. Conclusions

This study compared the gelation properties and microstructural characteristics among MPs from four types of meat sources. Among all the MPs, the PSM showed the most rigid and compact microstructure, followed by BSM, SSM, and FSM, at a concentration of 30 mg/mL. The SEM observation of gel microstructures indicated that the PSM gel had the finest network with the smallest voids. Conversely, open gel networks with large porosity were found in FSM gels. Moreover, SDS-PAGE revealed that the PSM had the highest amount of the MHC and actin. Rheological measurements indicated that fish proteins were inferior to those of mammalian proteins in terms of gel formation ability and gel strength. Studies on fish products should focus on improving the gel strength of fish protein. This study provided deeper understanding on gelation properties and microstructural characteristics of MPs from different animal sources, which is important for their applications in food products. Further studies are required to develop strategies for improving the gel strength of fish MP in order to achieve the similar gelation performance as mammalian MP gels.

Declaration of competing interest

The authors declare that they have no known competing financial interests or personal relationships that could have appeared to influence the work reported in this paper.

Abbreviations

MP	Myofibrillar protein
SDS-PAGE	Sodium dodecyl sulfate polyacrylamide gel electrophoresis
SEM	Scanning electron microscopy
FSM	Fish source MP
BSM	Beef source MP
SSM	Sheep source MP
PSM	Pork source MP
FSP	Fish source pieces
BSP	Beef source pieces
SSP	Sheep source pieces
PSP	Pork source pieces
MHC	the myosin heavy chain
MLC	the myosin light chains

Funding information

We gratefully acknowledge the support from the Natural Science Foundation of Zhejiang Province (LQ20C200011), National Key Research Program of China (2018YFD0401203), the Fundamental Research Funds for the Central Universities (Y0201700416), and National Natural Science Foundation of China (General Projects: 31871826).

Authors' contributions

Haifeng Wang, **Huijuan Yang**, **Zhi Yang** and **Qing Shen** conceived and designed the paper; **Haifeng Wang** and **Zhi Yang** collected and analysed the literature and wrote the paper; **Haifeng Wang**, **Huijuan Yang** and **Zhi Yang** edited the table and figures; **Haifeng Wang**, **Zhi Yang**, **Jing Xue**, **Yunyan Li**, **Shitong Wang**, **Lijun Ge**, and **Manman Zhang** reviewed and edited the manuscript. All authors read and approved the manuscript.

All applicable international, national, and/or institutional guidelines for the care and use of animals were followed. This article does not contain any studies with human participants performed by any of the authors.

References

Ahhmed, A. M., Kuroda, R., Kawaharas, S., et al. (2009). Dependence of microbial transglutaminase on meat type in myofibrillar proteins cross-linking. *Food Chemistry, 112*, 354–361. https://doi.org/10.1016/j.foodchem.2008.05.078. a1.

Antonov, Y. A., & Zhuravleva, I. L. (2019). Complexation of lysozyme with lambda carrageenan: Complex characterization and protein stability. *Food Hydrocolloids, 87*, 519–529. https://doi.org/10.1016/j.foodhyd.2018.08.040

Anvari, M., & Joyner Melito, H. S. (2017). Effect of fish gelatin-gum Arabic interactions on structural and functional properties of concentrated emulsions. *Food Research International, 102*, 1–7. https://doi.org/10.1016/j.foodres.2017.09.085

Baune, M. C., Schroeder, S., Witte, F., Heinz, V., & Terjung, N. (2021). Analysis of protein-network formation of different vegetable proteins during emulsification to produce solid fat substitutes. *Journal of Food Measurement and Characterization*, 1–18. https://doi.org/10.1007/S11694-020-00767-9

Bhat, F. Z., Morton, J. D., Mason, S. L., & Bekhit, A. E.-D. A. (2019). Pulsed electric field improved protein digestion of beef during in-vitro gastrointestinal simulation. *Lebensmittel-Wissenschaft und -Technologie- Food Science and Technology, 102*, 45–51. https://doi.org/10.1016/j.lwt.2018.12.013

Cai, L. Y., Wan, J. L., Li, X. X., & Li, J. R. (2020). Effects of different thawing methods on conformation and oxidation of myofibrillar protein from largemouth bass (Micropterus salmoides). *Journal of Food Science, 85*, 2470–2480. https://doi.org/10.1111/1750-3841.15336

Cao, H., Jiao, X., Fan, D., et al. (2019). Catalytic effect of transglutaminase mediated by myofibrillar protein crosslinking under microwave irradiation. *Food Chemistry, 284*, 45–52. https://doi.org/10.1016/j. foodchem.2019.01.097

Cao, Y., Ma, W., Huang, J., & Xiong, Y. L. (2020). Effects of sodium pyrophosphate coupled with catechin on the oxidative stability and gelling properties of myofibrillar protein. *Food Hydrocolloids, 104*, 1–9. https://doi.org/10.1016/j.foodhyd.2020. 105722

Chen, H. S., Diao, J. J., Li, Y. Y., et al. (2016). The effectiveness of clove extracts in the inhibition of hydroxyl radical oxidation-induced structural and rheological changes in porcine myofibrillar protein. *Meat Science, 111*, 60–66. https://doi.org/10.1016/j.meatsci.2015.08.017

Chen, X., Qiu, Q., Chen, K., Li, D., & Liang, L. (2020). Water-soluble myofibrillar protein-pectin complex for enhanced physical stability near the isoelectric point: Fabrication, rheology and thermal property. *International Journal of Biological Macromolecules, 142*, 615–623. https://doi.org/10.1016/j.ijbiomac.2019.10. 003

Consoli, L., Dias, R. A. O., Rabelo, R. S., et al. (2018). Sodium caseinate-corn starch hydrolysates conjugates obtained through the Maillard reaction as stabilizing agents in resveratrol-loaded emulsions. *Food Hydrocolloids, 84*, 458–472. https://doi.org/10.1016/j.foodhyd.2018.06.017

Cort, S.-R. A., Pacheco-aguilar, R., Elena, L.-S. N. M., et al. (2008). Production and functional evaluation of a protein concentrate from giant squid by acid dissolution and isoelectric precipitation. *Food Chemistry, 110*, 486–492. https://doi.org/10.1016/j.foodchem.2008.02.030

Dai, H. G., Sun, Y., Xia, W. Y., et al. (2021). Effect of phospholipids on the physicochemical properties of myofibrillar proteins solution mediated by NaCl concentration. *LWT-Food Science and Technology, 141*. https://doi.org/10.1016/j.lwt.2021.110895

Day, L., Xu, M., Oiseth, S. K., Lundin, L., & Hemar, Y. (2010). Dynamic rheological properties of plant cell-wall particle dispersions. *Colloids and Surfaces B: Biointerfaces, 81*, 461–467. https://doi.org/10.1016/j.colsurfb.2010.07.041

Elif, K., Ebru, K., Hichem, M., Senol, M., & Figen, Z. (2020). Extraction and characterization of novel multifunctional peptides from Trachinus Draco (greater weever) myofibrillar proteins with ACE/DPP4 inhibitory, antioxidant, and metal chelating activities. *Food Biochemistry, 22*, 1–9. https://doi.org/10.1111/jfbc.13179

Eysturskarð, J., Haug, I. J., Elharfaoui, N., Djabourov, M., & Draget, K. I. (2009). Structural and mechanical properties of fish gelatin as a function of extraction conditions. *Food Hydrocolloids, 23*, 1702–1711. https://doi.org/10.1016/j.foodhyd.2009.01.008

Fidalgo, L. G., Saraiva, J. A., Aubourg, S. P., & Vázquez, M. (2020). Changes on enzymatic activity and on sarcoplasmic and myofibrillar proteins of frozen-stored hake (Merluccius merluccius) pretreated by high pressure. *International Journal of Food Science and Technology, 55*, 2041–2048. https://doi.org/10.1111/ijfs.14395

Fu, Q., Liu, R., Wang, H., Hua, C., & Song, S. (2019). Effects of oxidation in vitro on structures and functions of myofibrillar protein from beef muscles. *Journal of Agricultural and Food Chemistry, 67*(20), pp5866–5873. https://doi.org/10.1021/acs.jafc.9b01239

Gabdukaeva, L. Z., Gumerov, T. Y., Nurgalieva, A. R., & Abdullina, L. V. (2021). IOP Conference Series: Earth and Environmental Science: Current trends in the development of functional meat products to improve the nutritional status of the population. In *International conference on world technological trends in agribusiness, omsk city, western Siberia*. Russian Federation. https://doi.org/10.1088/1755-1315/624/1/012196.

Gornall, A. G., Bardawill, C. J., & David, M. M. (1949). Determination of serum proteins by means of the biuret reaction. *Biochemistry, 177*, 751–766.
Grunert, K. G. (2006). Future trends and consumer lifestyles with regard to meat consumption. *Meat Science, 78*, 343–358. https://doi.org/10.1016/j.meatsci.2006.04.016
Hess, B. W., Moss, G. E., & Rule, D. C. (2008). A decade of developments in the area of fat supplementation research with beef cattle and sheep. *Journal of Animal Science*. https://doi.org/10.2527/jas.2007-0546
Hrynets, Y., Ndagijimana, M., & Betti, M. (2014). Transglutaminase-catalyzed glycosylation of natural actomyosin (NAM) using glucosamine as amine donor: Functionality and gel microstructure. *Food Hydrocolloids, 36*, 26–36. https://doi.org/10.1016/j.foodhyd.2013.09.001
Huang, T., Zhao, H., Fang, Y., et al. (2019). Comparison of gelling properties and flow behaviors of microbial transglutaminase (MTGase) and pectin modified fish gelatin. *Journal of Texture Studies, 50*, 400–409. https://doi.org/10.1111/jtxs.12405
Jia, N., Liu, D., Song, L., et al. (2019). The inhibition effect of gallic acid on oxidation of pork myofibrillar proteins and the crosslinking interaction between gallic acid and proteins. *Journal of Chinese Institute of Food Science and Technology, 19*, 12–19. https://doi.org/10.16429/j.1009-7848.2019.01.002
Jiang, L., & Wu, S. (2018). Pullulan suppresses the denaturation of myofibrillar protein of grass carp (Ctenopharyngodon idella) during frozen storage. *International Journal of Biological Macromolecules, 112*, 1171–1174. https://doi.org/10.1016/j.ijbiomac.2018.02.094
Komprda, T., Zelenka, J., Fajmonova, E., Bakaj, P., & Pechova, P. (2003). Cholesterol content in meat of some poultry and fish species as influenced by live weight and total lipid content. *Agricultural and Food Chemistry, 51*, 7692–7697. https://doi.org/10.1021/jf030378r
Laermmli, U. (1970). Cleavage of structural proteins during the assembly of the head of the bacteriophage T4. *Nature, 227*, 680–685. https://doi.org/10.1038/227680a0
Lametsch, R., Roepstorff, P., Moller, H. S., et al. (2004). Identification of myofibrillar substrates for calpain. *Meat Science, 68*, 515–521. https://doi.org/10.1016/j.meatsci.2004.03.018
Lee, C. H., & Chin, K. B. (2019). Changes in physicochemical properties of pork myofibrillar protein combined with corn starch and application to low-fat pork patties. *International Journal of Food Science and Technology, 55*, 157–164. https://doi.org/10.1111/ijfs.14272
Li, K., Fu, L., Zhao, Y.-Y., et al. (2020a). Use of high-intensity ultrasound to improve emulsifying properties of chicken myofibrillar protein and enhance the rheological properties and stability of the emulsion. *Food Hydrocolloids, 98*, 105275. https://doi.org/10.1016/j.foodhyd.2019.105275
Li, K., Li, Y., Kang, C., et al. (2020b). Effect of atmospheric pressure plasma jet on structural and rheological properties of chicken myofibrillar protein. *Food Science, 41*(19), 124–131. https://doi.org/10.7506/spkx1002-6630-20190916-202
Lin, D., Zhang, L., Li, R., et al. (2019). Effect of plant protein mixtures on the microstructure and rheological properties of myofibrillar protein gel derived from red sea bream (Pagrosomus major). *Food Hydrocolloids, 96*, 537–545. https://doi.org/10.1016/j.foodhyd.2019. 05.043
Liu, Z. Y., Liu, Y., & Luo, C. (2015). Effect of tea polyphenols on grass carp rheological characteristics. *Modern Food Science and Technology, 31*, 50–58. https://doi.org/10.13982/j.mfst.1673-9078.2015.6.009
Liu, C., Li, W., & Zhou, M. (2021). Effect of oxidation modification induced by peroxyl radicals on the physicochemical and gel characteristics of grass carp myofibrillar protein. *Journal of Food Measurement and Characterization*. https://doi.org/10.1007/s11694-021-01123-1
Li, F. F., Wang, B., Liu, Q., et al. (2019). Changes in myofibrillar protein gel quality of porcine longissimus muscle induced by its stuctural modification under different thawing methods. *Meat Science, 147*, 108–115. https://doi.org/10.1016/j.meatsci.2018.09.003
Mahmudul, M. H., Vipasha, S., Chyngyz, E., et al. (2021). Principal component analysis of lipid and protein oxidation products and their impact on color stability in bison longissimus lumborum and psoas major muscles. *Meat Science, 178*, 108523. https://doi.org/10.1016/j.meatsci.2021.108523
Malva, A. D., Albenzio, M., Santillo, A., et al. (2018). Methods for extraction of muscle proteins from meat and fish using denaturing and nondenaturing solutions. *Journal of Food Quality*. https://doi.org/10.1155/2018/8478471, 2018.
Miller, D. K., Acevedo, N. C., Lonergan, J. G., Sebranek, J. G., & Tarté, R. (2019). Rheological characteristics of mechanically separated chicken and chicken breast trim myofibril solutions during thermal gelation. *Food Chemistry, 307*. https://doi.org/10.1016/j.foodchem.2019.125557
Raei, M., Rafe, A., & Shahidi, F. (2018). Rheological and structural characteristics of whey protein-pectin complex coacervates. *Journal of Food Engineering, 228*, 25–31. https://doi.org/10.1016/j.jfoodeng.2018.02.007
Romani, V. P., Machado, A. V., Olsen, B. D., & Martins, V. G. (2018). Effects of pH modification in proteins from fish (Whitemouth croaker) and their application in food packaging films. *Food Hydrocolloids, 74*, 307–314. https://doi.org/10.1016/j.foodhyd.2017.08.021
Sano, T., Noguchi, S. F., & Tauchiya, T. (1988). Dynamic viscoelastic behavior of natural actomyosin and myosin during thermal gelation. *Journal of Food Science, 53*, 924–928. https://doi.org/10.1111/j.1365-2621.1988.tb08987.x
Shan, L. Y., Li, Y., Wang, Q., et al. (2020). Profiles of gelling characteristics of myofibrillar proteins extracted from chicken breast: Effects of temperatures and phosphates. *LWT-Food Science and Technology, 129*. https://doi.org/10.1016/j.lwt.2020.109525
Shi, H. N., Zhang, M. L., Zhang, J., et al. (2021). Effect of nano fish bone on myosin gel properties of silver carp. *Food Science, 42*, 71–76. http://kns.cnki.net/kcms/detail/11.2206.TS.20200416.1826.008.html.
Shi, H., Zhou, T., Wang, X., et al. (2021). Effects of the structure and gel properties of myofibrillar protein on chicken breast quality treated with ultrasound-assisted potassium alginate. *Food Chemistry, 358*. https://doi.org/10.1016/j.foodchem.2021.129873
Siong, H. T., Rodney, J. M., Christopher, L. B., Samson, O. A., & Li, D. (2014). Gelling properties of protein fractions and protein isolate extracted from Australian canola meal. *Food Research International, 62*, 819–828. https://doi.org/10.1016/j.foodres.2014.04.055
Tang, C. H., & Liu, F. (2013). Cold, gel-like soy protein emulsions by micro-fluidization: Emulsion characteristics, rheological and microstructural properties, and gelling mechanism. *Food Hydrocolloids, 30*, 61–72. https://doi.org/10.1016/j.foodhyd.2012.05.008
Wang, Q. (2014). Detection and profiling of fatty acids of inner Mongolian beef and mutton. College of food science and engineering. *Food Hydrocolloids, 107*, 105920. https://doi.org/10.1016/j.foodhyd.2020.105920
Wang, Y., Eastwood, B., Yang, Z., et al. (2019). Rheological and structural characterization of acidified skim milks and infant formulae made from cow and goat milk. *Food Hydrocolloids, 96*, 161–170. https://doi.org/10.1016/j.foodhyd.2019.05.020
Wang, L. M., Xia, M. Q., Zhou, Y., et al. (2020). Gel properties of grass carp myofibrillar protein modified by low-frequency magnetic field during two-stage water bath heating. *Food Hydrocolloids, 107*. https://doi.org/10.1016/j.foodhyd.2020.105920
Wang, L., Xiong, G. Q., Peng, Y. B., et al. (2014). The cryoprotective effect of different konjac glucomannan (KGM) hydrolysates on the glass carp (Ctenopharygodon idella) myofibrillar during frozen storage. *Food and Bioprocess Technology, 7*(12), 3398–3406. https://doi.org/10.1007/s11947-014-1345-3
Wei, S., Yang, Y., Feng, X., et al. (2020). Structures and properties of chicken myofibrillar protein gel induced by microwave heating. *International Journal of Food Science and Technology, 55*, 2691–2699. https://doi.org/10.1111/ijfs.14522
Westphalen, A., Briggs, J., & Lonergan, S. (2006). Influence of muscle type on rheological properties of porcine myofibrillar protein during heat-induced gelation. *Meat Science, 72*, 697–703. https://doi.org/10.1016/j.meatsci.2005.09.021
Wood, J. D., Enser, M., Nute, A. V., et al. (2008). Fat deposition, fatty acid composition and meat quality: A review. *Meat Science, 78*, 343–358. https://doi.org/10.1016/j.meatsci.2007.07.019
Xu, X. J., Xu, J., Zhang, Y. Y., & Zhang, L. N. (2008). Rheology of triple helical Lentinan in solution: Steady shear viscosity and dynamic oscillatory behavior. *Food Hydrocolloids, 22*, 735–741. https://doi.org/10.1016/j.foodhyd.2007.02.010
Xu, Y. J., Zhao, Y. Q., Wei, Z. X., et al. (2020). Modification of myofibrillar protein via glycation: Physicochemical characterization, rheological behavior and solubility property. *Food Hydrocolloids, 105*, 1–39. https://doi.org/10.1016/j.foodhyd.2020.105852
Yang, Z., Hemar, Y., Hilliou, L., et al. (2016). Nonlinear behavior of gelatin networks reveals a hierarchical structure. *Biomacromolecules, 17*(2), 590–600. https://doi.org/10.1021/acs.biomac.5b01538
Yang, H. H., Zhong, C., Sun, L. C., et al. (2021). Effects of partial substitution of NaCl on myofibrillar protein properties from pearl mussel Hyriopsis cumingii muscle: Structural characteristics and aggregation behaviors. *Food Chemistry, 356*, 129734. https://doi.org/10.1016/J.FOODCHEM.2021.129734
Yang, X., & Zhang, Y. (2019). Expression of recombinant transglutaminase gene in Pichia pastorisand its uses in restructured meat products. *Food Chemistry, 291*, 245–252. https://doi.org/10.1016/j.foodchem.2019.04.015
Zhang, L., Li, Q., Shi, J., Zhu, B., & Luo, Y. (2017). Changes in chemical interactions and gel properties of heat-induced surimi gels from silver carp (Hypophthalmichthys molitrix) fillets during setting and heating: Effects of different washing solutions. *Food Hydrocolloids, 75*, 116–124. https://doi.org/10.1016/j.foodhyd.2017.09.007
Zheng, J., Han, Y., Ge, G., Zhao, M., & Sun, W. (2019). Partial substitution of NaCl with chloride salt mixtures: Impact on oxidative characteristics of meat myofibrillar protein and their rheological properties. *Food Hydrocolloids, 96*, 36–42. https://doi.org/10.1016/j.foodhyd.2019.05.003
Zhou, X. X., Liu, H. H., Zhu, S. C., et al. (2020). Textural, rheological and chemical properties of surimi nutritionally-enhanced with lecithin. *LWT-Food Science & Technology, 122*, 108984. https://doi.org/10.1016/j.lwt.2019.108984
Zhou, R., Ni, Q., Lin, W., et al. (2015). The dependency of the myofibrils solubility on the ion concentration. *Journal of Chinese Institute of Food Science and Technology, 15*(3), 32–39. https://doi.org/10.16429/j.10097848.2015.03.005
Zhou, L., Yang, Y. L., Wang, J. Y., Wei, S. M., & Li, S. S. (2018). Effect of low fat addition on chicken myofibrillar protein gelation properties. *Food Hydrocolloids, 90*, 4785. https://doi.org/10.1016/j.foodhyd.2018.11.044
Zhu, Y. D., Li, D., & Wang, L. J. (2018). Dynamic rheological properties of peanut protein isolate and aggregation suspension and acid-induced gel. *Power Technology, 358*, 95–102. https://doi.org/10.1016/j.powtec.2018.08.052
Zilhadia, I. (2013). *Protein Profilesof Beef (Bos indicus), Pork (Sus domesticus), and SausagesBy Using SDS-PAGE (Sodium Dodecyl Sulphate Polyacrylamide Gel Electrophoresis) Method*. University of california press. https://doi.org/10.2307/25157345